DTU Library

D6.4 Impact assessment: KPIs evolution in Bornholm

Zepter, Jan Martin; Engelhardt, Jan; Marinelli, Mattia

Publication date:
2023

Document Version
Publisher's PDF, also known as Version of record

D6.4 Impact assessment: KPIs evolution in Bornholm

WP6 – Demonstration in Bornholm

INSULAE
Maximizing the impact of innovative energy approaches in the EU islands

Prepared by Jan Martin Zepter, Jan Engelhardt, and Mattia Marinelli (DTU)

Date: 16/10/2023

This project has received funding from the European Union's Horizon 2020 research and innovation programme under Grant Agreement No 824433

DELIVERABLE FACTSHEET

Document Name:	D6.4 Impact assessment: KPIs evolution in Bornholm
Responsible Partner:	DTU
WP:	WP6 – Demonstration in Bornholm
Task:	T6.4 Evaluation and impact assessment
Deliverable nº:	6.4

Approvals

Dissemination level	
	PU = Public
	PP = Restricted to other programme participants (including the EC)
	RE = Restricted to a group specified by the consortium (including the EC)
X	CO = Confidential, only for members of the consortium (including the EC)

	Company
Author(s)	DTU
Task Leader	DTU
WP Leader	DTU

Documents history

Revision	Date	Main modification	Author
1	15/08/2022	First table of contents	DTU
2	15/05/2023	First draft	DTU
3	11/09/2023	Final draft	DTU
4	16/10/2023	Final version after revision	DTU/CIRCE/CERTH

DISCLAIMER OF WARRANTIES

"This project has received funding from the European Union's Horizon 2020 research and innovation programme under Grant Agreement No 824433".

This document has been prepared by INSULAE project partners as an account of work carried out within the framework of the EC-GA contract no 824433.

Neither Project Coordinator, nor any signatory party of INSULAE Project Consortium Agreement, nor any person acting on behalf of any of them:

(a) makes any warranty or representation whatsoever, express or implied,
   (i). with respect to the use of any information, apparatus, method, process, or similar item disclosed in this document, including merchantability and fitness for a particular purpose, or
   (ii). that such use does not infringe on or interfere with privately owned rights, including any party's intellectual property, or
   (iii). that this document is suitable to any particular user's circumstance; or

(b) assumes responsibility for any damages or other liability whatsoever (including any consequential damages, even if Project Coordinator or any representative of a signatory party of the INSULAE Project Consortium Agreement, has been advised of the possibility of such damages) resulting from your selection or use of this document or any information, apparatus, method, process, or similar item disclosed in this document.

ABBREVIATIONS

APC	Active power control
BESS	Battery energy storage system
BMS	Battery management system
CCS	Combined charging system
CHP	Combined heat and power
DER	Distributed energy resource
DHP	District heating plant
DSO	Distribution system operator
EMS	Energy management system
EV	Electric vehicles
HCS	Hybrid charging system
HPC	High-power charger
ICE	Internal combustion engine
KPI	Key performance indicator
MeOH	Methanol
MPPT	Maximum power point tracking
PV	Photovoltaic
RES	Renewable energy sources
SNG	Synthetic natural gas
SMR	Steam methane reforming
SOC	State of charge
SOH	State of health
UCs	Use cases
VPP	Virtual power plant

EXECUTIVE SUMMARY

This deliverable assesses the impact of several key performance indicators (KPIs) for the demonstration activities carried out in Use Cases (UCs) 4 and 5 in the Lighthouse Island of Bornholm.

Use Case 4 demonstrated the feasibility of a DC microgrid acting as a hybrid fast charging station for electric vehicles. This deployed intervention featured a novel battery system architecture and a photovoltaic installation, and was located at an educational institute in Rønne on Bornholm over a period of 15 months. This report gathers the main numerical outcomes and analyses the impact on key metrics such as EV charging fulfillment, carbon emission reduction, and self-sufficiency. Over the entire demonstration phase with this hybrid charging station (HCS), 2008 EV charging sessions were recorded, amounting to a total charged energy of 21.8 MWh. An overall proportion of 37.7% of the energy delivered to EVs was provided by the local PV system, defining the system's self-sufficiency. Furthermore, 90% of the total energy provided by the local PV system was utilized for EV charging, defining the system's self-consumption. The operational CO_2 emissions of the HCS amounted to $2092\,\mathrm{kg}_{\mathrm{CO_2}}$, which is a reduction of around 1 ton CO_2 compared to a charging system without local PV system ($3{,}094\,\mathrm{kg}_{\mathrm{CO_2}}$), and a reduction of 14.5 tons CO_2 compared to the emissions caused by ICE vehicles ($17{,}649\,\mathrm{kg}_{\mathrm{CO_2}}$).

Use Case 5 aimed at demonstrating flexibility aspects of distributed generation units to support the electrical, thermal, and transportation sectors. The focus of the investigation has been a biogas plant located in Aakirkeby, Bornholm, both for simulation studies and experimental tests. Moreover, the controllability of other distributed generation units, such as wind and solar PV, has been experimentally assessed within the demonstration activities. The last part was concerned with more hypothetical scenarios of how different units located at the substation of Aakirkeby could be coordinated together to supply multi-energy demands. The different analyses in UC5 showed that currently deployed units already provide high potential for short-term flexibility activations. For islands, the ferry connection to the mainland is often one of the biggest contributors of CO_2 emissions. Here, hydrogen may play a significant role in helping decarbonise this means of transport, either directly or through hydrogen-based derivatives. The work in UC5 demonstrates that electrolysers integrate well into the thermal and electrical energy balances, while providing hydrogen for hard-to-electrify applications. Yet, the local production of hydrogen/methanol could only provide a small share of the ferries' demand on Bornholm, without a strong expansion of renewable generation capacity.

TABLE OF CONTENTS

1 Introduction....1

1.1 UC4 – Transition to DC grids....1

1.2 UC5 – Local bio-based economies supporting the electrical, thermal and transport systems integrated management....2

2 Impact assessment for use case #4 – Transition to DC grids....3

2.1 Definition of KPIs....3

2.1.1 Data acquisition....3

2.1.2 Data analysis....3

2.1.3 Summary of KPIs....3

2.2 Evaluation of KPIs....4

2.2.1 Summary of operational results....4

2.2.2 EV charging behaviour....5

2.2.3 Carbon emissions....7

2.2.4 Daily progressions....8

2.2.5 Operating and investment expenditures....10

3 Impact assessment for use case #5 – Local bio-based economies supporting the electrical, thermal and transport systems integrated management....14

3.1 Definition of KPIs....14

3.1.1 Operational flexibility....14

3.1.2 Biogas and methanol production....15

3.1.3 Multi-energy coordination at substation level....16

3.2 Evaluation of KPIs....17

3.2.1 Assessment of operational flexibility....17

3.2.2 Assessment of biogas and methanol production....22

3.2.3 Assessment of multi-energy coordination at substation level....25

4 Conclusions....28

References....30

1 INTRODUCTION

Task 6.4 was dedicated to preparatory activities for performing a comprehensive analysis of the medium and long-term impacts of the interventions implemented on the Lighthouse Island Bornholm. To this end, this deliverable provides an exhaustive analysis of the key results from the interventions implemented on Bornholm. The focus is set on describing the operating results and main insights from the conducted analyses with respect to defined key performance indicators (KPIs) for the two respective Use Cases (UCs) investigated on Bornholm. Section 1.1 details the main content of UC4, while Section 1.2 presents the general focus of work in UC5.

1.1 UC4 – Transition to DC grids

Within UC4, a prototype of a DC microgrid has been developed and installed at Campus Bornholm, an educational institution in the main town, Rønne. The setup comprises a novel type of battery system (312 kWh), two 175 kW EV fast chargers, a 61 kWp PV installation, and a 43 kW connection to the local AC distribution grid. In the following, this system will be referred to as a hybrid charging system (HCS). Figure 1 provides a schematic overview of the HCS. The BESS, as a power and energy buffer, facilitates full usage of the power capability of both the PV system and EV chargers, despite the grid capacity being lower rated than the system components. The energy storage consists of three reconfigurable battery strings of 104 kWh each, which have the intrinsic capability to control their voltage during operation [2]. This allows them to directly connect to the other system components without the need for interfacing power converters [3][4].

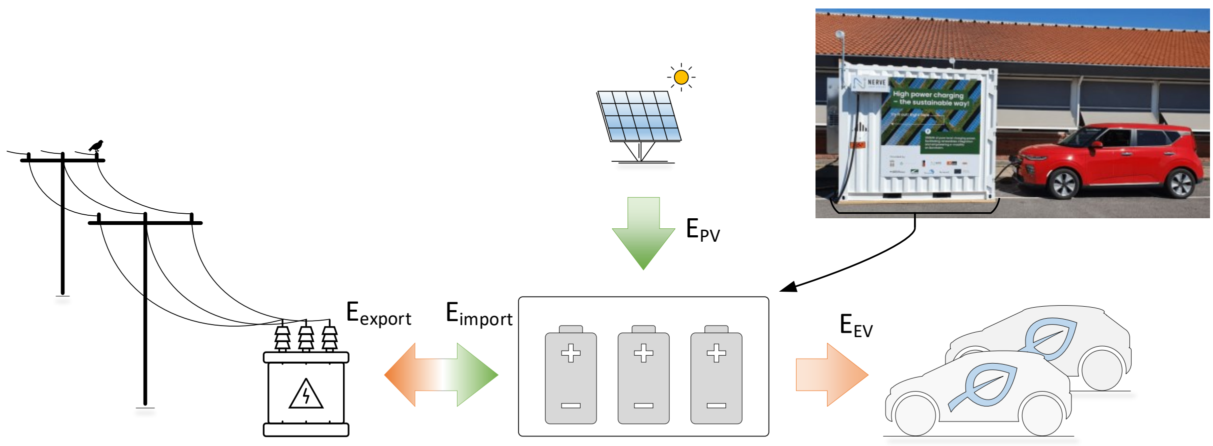

Figure 1: Overview of the hybrid EV fast charging system on the island of Bornholm.

In July 2021, the HCS was deployed in the parking lot of Campus Bornholm. This location offered public access to the two fast chargers, and charging was free of cost. The prototype was in operation for more than one year, before being eventually decommissioned in September 2022. While the EV chargers were accessible throughout the entire period, the grid export of excess PV energy was only possible from May 2022, since this operation required permission from the grid operator. Section 2 summarizes the operational results for the demonstration phase of UC4.

1.2 UC5 – Local bio-based economies supporting the electrical, thermal and transport systems integrated management

Use Case 5 has been focusing on the increase of local bio-based generation for supporting the electrical, thermal and transport systems on the island of Bornholm. In particular, the core of the investigation was to understand the capability of the biogas plant at the substation of Aakirkeby to provide flexible combined heat and power production in the context of establishing a virtual power plant (VPP), see Figure 2. In this regard, several experimental tests have been carried with the biogas plant to analyse relevant KPIs for the joint operation with local renewable energy sources (RES). As UC5 did not introduce one specific technological intervention, the conducted activities aimed at the experimental demonstration with local units in Bornholm. The modelling and demonstration plans have been presented in deliverable D6.1, while this deliverable at hand summarises the main KPIs and associated results. Section 3 gathers the relevant quantitative results from the conducted experiments and simulations.

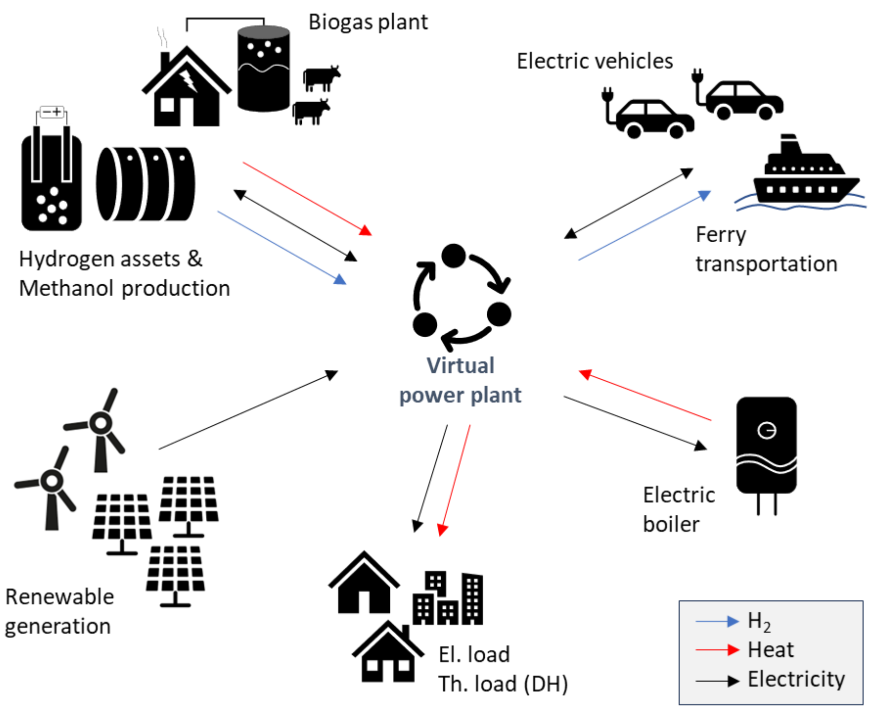

Figure 2: Virtual power plant with electrical, thermal and heat flows indicated.

2 Impact assessment for use case #4 – Transition to DC grids

The impact assessment for UC 4 is structured in two main sections. Section 2.1 provides details on data acquisition throughout the demonstration phase and defines the KPIs for this use case. Subsequently, Section 2.2 assesses the impact of UC4 based on the defined KPIs.

2.1 Definition of KPIs

2.1.1 Data acquisition

For the demonstration phase of the prototype being in operation from July 2021 to September 2022, the HCS was monitored in high resolution with recorded measurements at all system components. Specifically, the PV production was measured together with the solar irradiation at the site in second-based resolution. The power flowing from and to the battery system was measured together with the string connection to the individual units as well as the state-of-charge levels of the battery strings. This allowed for estimating the energy that was sent to the grid, imported from the grid, stored, or charged to the EVs. The EV charging data obtained at the demonstration site cover arrival and departure times as well as charging progressions of individual charging sessions. Moreover, electricity meters were installed at the point of connection of the HCS monitoring the actual imported and exported energy to the grid and providing information on the system's auxiliary consumption for thermal management.

2.1.2 Data analysis

The acquired measurements were analyzed to assess the performance of the HCS with respect to several key performance indicators. The energy flows from and to the system components were examined, both in absolute numbers for the full demonstration period and average hourly progressions over a day. From these energy flows, the system's self-sufficiency and self-consumption can be calculated, describing how well the system is able to satisfy own demand (EV charging) from own local production. These metrics are key for assessing such HCS solutions with own production unit and storage. In addition, the charging behavior at the HCS has been analyzed with respect to the distribution of charging sessions over the total demonstration period as well as during the day. The recorded data further allowed to determine the operational CO_2 emission reduction introduced by the HCS solution, compared with the similar energy requirement from gasoline cars as well as EVs charged solely from the grid with an average emission factor. Finally, the analysis includes an estimation of operational and investment expenditures.

2.1.3 Summary of KPIs

The following list provides an overview of all KPIs that were assessed for UC 4:

- Energy produced by the PV installation (kWh)
- Energy delivered to EVs charging at the HCS (kWh)
- Energy imported from the grid (kWh)
- Energy exported to the grid (kWh)
- Self-sufficiency of the HCS (%)
- Self-consumption of the HCS (%)
- Operational CO_2 emissions of the HCS ($\mathrm{kg}_{\mathrm{CO}_2}$)
- Number of charging sessions, per month and daily distribution (#)
- Energy of individual charging sessions (kWh)
- Power (average & peak) of individual charging sessions (kW)
- Operational expenditures (€)
- Investment expenditures (€)

Each of the listed KPIs will be addressed in detail in the following section.

2.2 Evaluation of KPIs

2.2.1 Summary of operational results

The HCS was operational between July 2021 and September 2022. Table 1 gathers the overall operational results of the system operation by years. During this testing period, a total number of 2008 EVs was charged from the battery. The table summarizes the energy provided to the EVs, energy exported from the HCS to the grid, energy harvested from the local PV system, and energy imported from the grid. In the beginning of the demonstration phase, energy export to the grid as well as the capabilities of harvesting PV energy were not fully operational, leading to lower-than-expected values. Hence, more energy had to be relatively imported to substitute missing PV energy. In 2022, significantly more PV energy was utilized in the HCS. Similarly, the amount of energy charged to EVs increased in 2022 due to more charging sessions taking place, as discussed in the next subsection.

Table 1: Overall energy inputs and outputs of the HCS prototype for the complete demonstration phase.

Year	E_{EV} (kWh)	E_{export} (kWh)	E_{PV} (kWh)	E_{import} (kWh)
2021	4,891	0	491	5,253
2022	16,899	2,418	9,260	10,861
Total	21,790	2,418	9,751	16,114

For an HCS, self-sufficiency is an important metric detailing how much of the local consumption, i.e., in this case the EV charging, was met by the local PV system. Zepter et al. [5] derive how to calculate self-sufficiency in systems with energy storage. Applying the formula for the self-sufficiency ratio (SSR), as in (1), yields:

$$SSR = \frac{E_{PV}}{E_{PV} + E_{import}} \cdot 100\% = 37.7\%, \quad (1)$$

signifying that 37.7% of the local demand was met by the local PV system for the whole demonstration period. Besides self-sufficiency, the self-consumption ratio (SCR) determines the amount of PV energy that was utilized for local demand, and it calculates as

$$SCR = \frac{E_{EV}}{E_{EV} + E_{export}} \cdot 100\% = 90.0\%. \quad (2)$$

Thus, 90% of the local generation has been used for EV charging.

The overall roundtrip battery system efficiency has been calculated to be 93.5%, based on the difference between energy inputs and outputs of the battery strings. On top of that, the HCS entails losses for auxiliary consumption connected to the thermal management system, controller consumption, and inverter losses, which is further addressed in the analysis of operating costs.

2.2.2 EV charging behaviour

The operation of the HCS employed by the energy management system (EMS) is strongly influenced by the behavior of EV users. Therefore, this section aims to provide a quantitative evaluation of how EV charging has been distributed over the operational lifetime of the battery system.

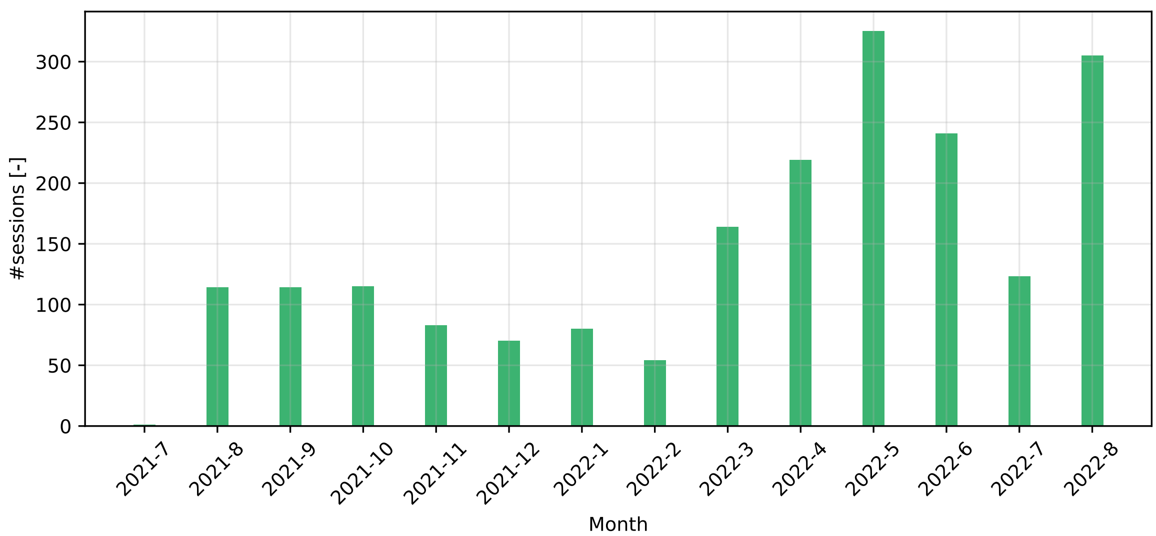

Figure 3: Monthly number of EV charging sessions throughout the demonstration phase.

Figure 3 provides an overview of the monthly distribution of electric vehicle (EV) charging sessions. The battery energy storage system (BESS) was deployed in July 2021 and, after initial tests, was made publicly accessible with charging being free of cost. The general data logging system was eventually activated from August which allowed for analyzing the system performance remotely. All in all, the number of charging sessions increased over the operational lifetime of the system, due to increasing awareness among the island's residents of the existence and location of the HCS. Initially, during autumn and winter, the number of charging sessions decreased until, in March 2022, the monthly charging sessions began to significantly increase, with a peak observed in May 2022. Another decline in charging sessions was noted during July 2022. This trend may be caused by lower presence of residents during Danish summer holidays, as well as by reduced system availability due to software updates and maintenance during this period. Finally, charging sessions returned to approximately 300 per month in August 2022.

Figure 4 illustrates the distribution of all EV charging sessions throughout the day. In total, 2008 EV charging sessions were recorded throughout the entire demonstration phase of the project. The figure shows that the majority of EV charging activity occurs between 8 a.m. and 9 p.m., with the highest utilization occurring in the afternoon. On the one hand, this trend can partially be attributed to location-specific reasons, since the HCS was installed at the parking lot of the educational institution Campus Bornholm, with nearby sports facilities. Thus, visitors to the school are expected to use the battery system for EV charging during daytime and evening hours. On the other hand, the observed general charging pattern with minimal activity during night-time hours also matches with previous research on fast charger utilization [6], and might therefore not be entirely specific to the location.

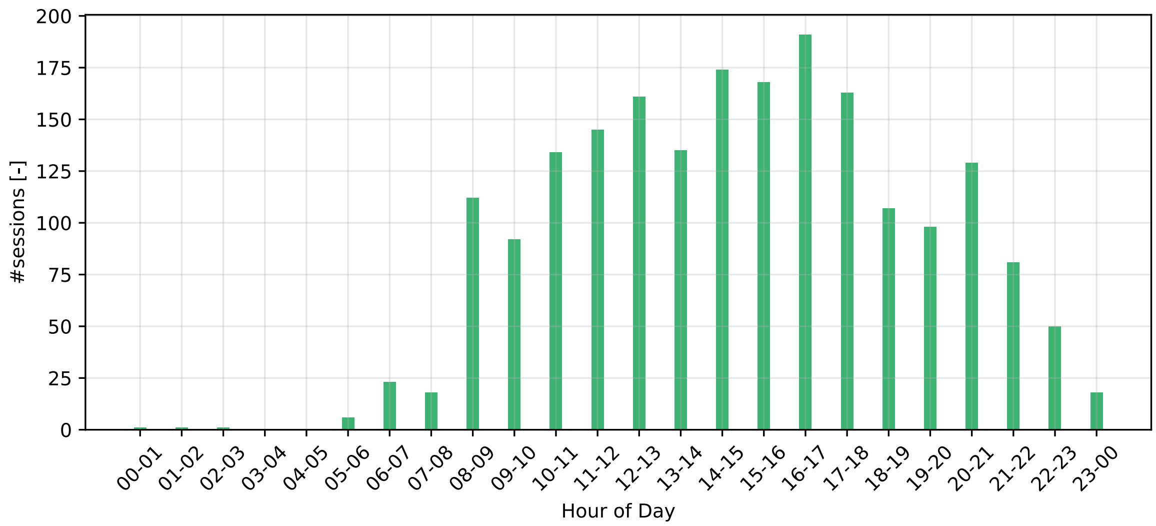

Figure 4: Hourly distribution of EV charging sessions throughout the day.

The high-resolution data logging further allowed to investigate the power and energy relations of individual charging sessions. To this end, a data subset of 751 charging events was analysed [7]: Figure 5 provides an overview of all charging events, represented as scatter plots for average power and charged energy in subfigure (a), and average and maximum power in subfigure (b).

Although EVs with a large battery capacity tend to also have a higher power capability, the comparison of observed power and energy values does not reveal a strong correlation in this regard. However, one striking aspect of the data is that many sessions ended with only little transferred energy. The predominant reason for this observation is that, particularly in the first months, the prototype did not control the charging current with necessary accuracy, as required by charging standard IEC61851:23 [3]. As a result, EVs prematurely terminated the charging process shortly after the start, resulting in numerous events with only marginal energy transfer. Additionally, location-specific reasons for charging durations of only a few minutes cannot be ruled out. The mean of the average charging power of all events is 53 kW, with 68 % having an average power between 25 kW and 80 kW. The maximum charged energy is 65 kWh, and the maximum average power 140 kW. The comparison of average and maximum power shows a clear correlation. All data points are in the upper triangle of the plot above the line of equality, since the maximum power during a charging process is naturally larger or equal to the average power. From all charging events, 82 % had a maximum power above the grid capacity of 43 kW, 25 % above 100 kW, and 12 % above 125 kW. The maximum EV power observed at the prototype was 166 kW.

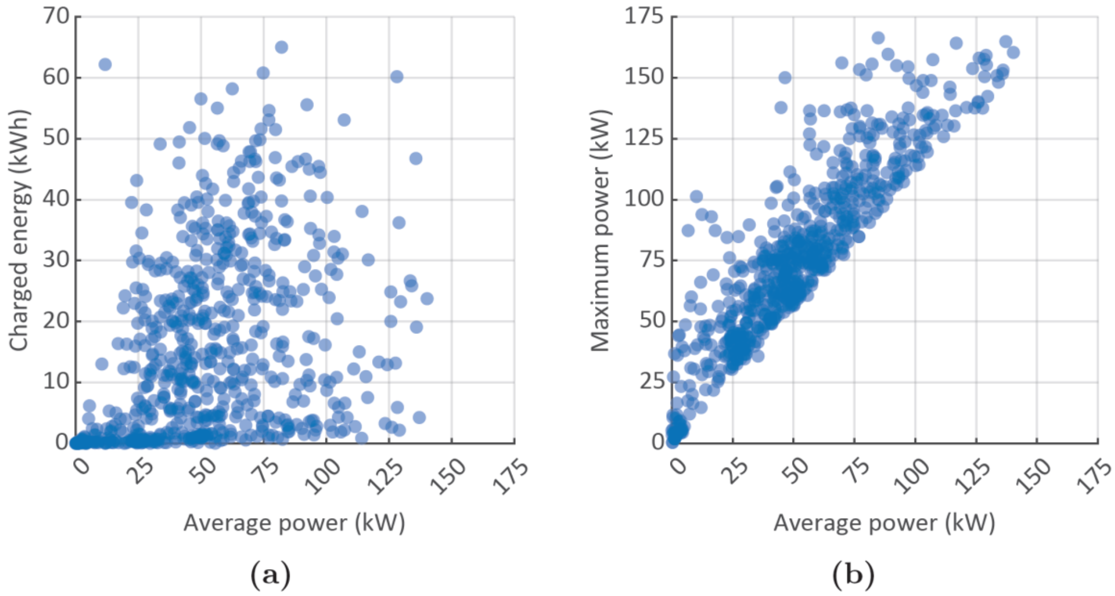

Figure 5: Charging data recorded at the demonstration site on Bornholm: (a) average power and charged energy of individual charging events; (b) average and maximum charging power of individual charging events.

2.2.3 Carbon emissions

The following section establishes the reductions in carbon emissions from EVs powered by the battery system compared to vehicles with an ICE, and EVs powered by direct grid charge. The total EV demand from Table 1 is used to determine the total driving distance by EVs assuming an average consumption of 0.2 kWh/km [8]:

$$D_{EV} = \frac{E_{EV}}{r_{EV}} = \frac{21{,}790 \text{ kWh}}{0.2 \frac{\text{kWh}}{\text{km}}} = 108{,}950 \text{ km} \tag{3}$$

Considering an average consumption rate of 15 km/l, a vehicle with an ICE consumes 7,263 l of gasoline to cover 108.950 km:

$$C_{ICE,petrol} = \frac{D_{EV}}{r_{ice}} = \frac{108{,}950 \text{ km}}{15 \frac{\text{km}}{\text{l}}} = 7{,}263 \text{ l} \tag{4}$$

The emission rate from an ICE is estimated to be 2.43 kg_{co_2}/l [9], yielding total emissions of:

$$\Upsilon_{ICE} = C_{ICE,petrol} \cdot \epsilon_{petrol} = 7{,}263 \text{ l} \cdot 2.43 \frac{\text{kg}_{\text{CO}_2}}{\text{l}} = 17{,}649 \text{ kg}_{\text{CO}_2} \tag{5}$$

When taking into consideration the emission factor of the Danish electricity grid of 0.142 kg_{co_2}/kWh in 2021 [10], the total emissions if the grid was to cover the whole EV demand are:

$$\Upsilon_{grid} = E_{EV} \cdot \epsilon_{grid} = 21{,}790 \text{ kWh} \cdot 0.142 \frac{\text{kg}_{\text{CO}_2}}{\text{kWh}} = 3{,}094 \text{ kg}_{\text{CO}_2} \tag{6}$$

The HCS under investigation is also connected to a rooftop PV system. Assuming a CO_2 emission rate of 0.02 kg_{co_2}/kWh for the PV installation [11] and a SSR of 37.7% for the HCS, the combined emissions from using the local PV system and the Danish grid for the EV demand reduce even further:

$$\Upsilon_{battery} = E_{EV} \cdot [SSR \cdot \epsilon_{PV} + (1 - SSR) \cdot \epsilon_{grid}] = 2092 \text{ kg}_{\text{CO}_2} \tag{7}$$

The results above are derived using the values in Table 1 for PV production and imported energy during the operational demonstration. Comparing EV charging from grid to the ICE emissions, a reduction of approximately 14.5 tons CO_2 is achieved. An additional reduction of around 1000 kg CO_2 is achieved when PV energy is integrated into the HCS.

2.2.4 Daily progressions

During the demonstration phase, there have been periods with down-time due to hardware replacement, maintenance, or pending approvals by the grid operator. In fact, the three months from June – August 2022 is the only period where all EMS and BESS functionalities were fully activated. Before June, excess PV energy could not be exported. Instead, the PV would simply be curtailed if the battery was already fully charged. For this reason, the following section will only present results for the three-month period with full EMS functionality.

Figure 6 and Figure 7 display daily average progressions of exported, imported, PV and EV energy. The two plots are divided into the system's energy outputs and inputs, respectively. The first plot supports the observations made from the section on EV sessions, as EV energy is consumed primarily between 8 a.m. and 9 p.m. PV energy is only available during daytime and this trend is also present for hours with exported energy.

As seen from the plot, the EMS slightly delays the export of excess PV energy in anticipation of a higher EV demand during daytime. One noteworthy characteristic of the EV demand is the local peak of charged energy in the period 8 p.m. – 9 p.m. This location-specific charging behavior was previously discussed by Bowen et al. [12].

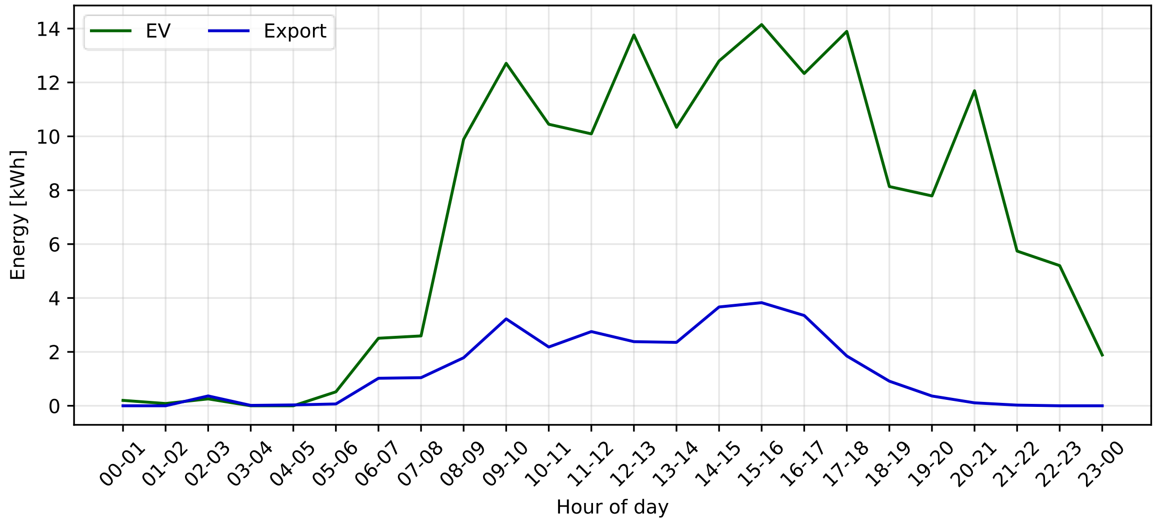

Figure 6: Average daily profile of system energy outputs comprising EV charging and grid export.

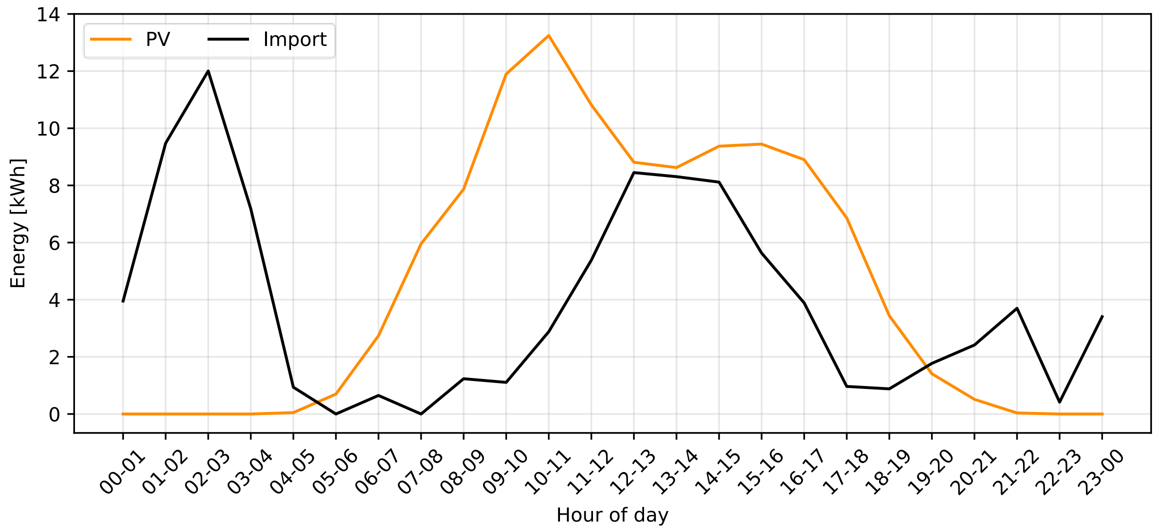

Figure 7: Average daily profile of system energy inputs comprising PV production and grid import.

In Figure 7, the average daily progression of imported energy has two larger peaks. The first peak occurs during the night and the second peak during the early afternoon. The EMS selects these time periods for grid imports based on the progression of spot prices. To clarify this point, Figure 8 presents an overview of the daily spot price profile by quarter during the operational lifetime of the system. These profiles show a clear trend in prices levels throughout the day. Prices peak in the morning and then again in the late afternoon. Furthermore, the general price level has increased throughout the operational period with average daily prices in 2022-Q3 three times higher than in 2021-Q3. The EMS specifically utilizes time windows with low spot prices to import energy if PV production is low or EV demand is high. In case the battery storage was solely used to perform energy arbitrage, the progression for the exported energy in Figure 6 would closely follow the spot price profile in Figure 8, for maximizing revenue. However, the EMS objectives are defined such that PV production is stored and used to cover the EV demand. Thus, the exported energy has a similar daily profile as PV production, since grid export only occurs when the battery is fully charged, and there is an excess of PV production.

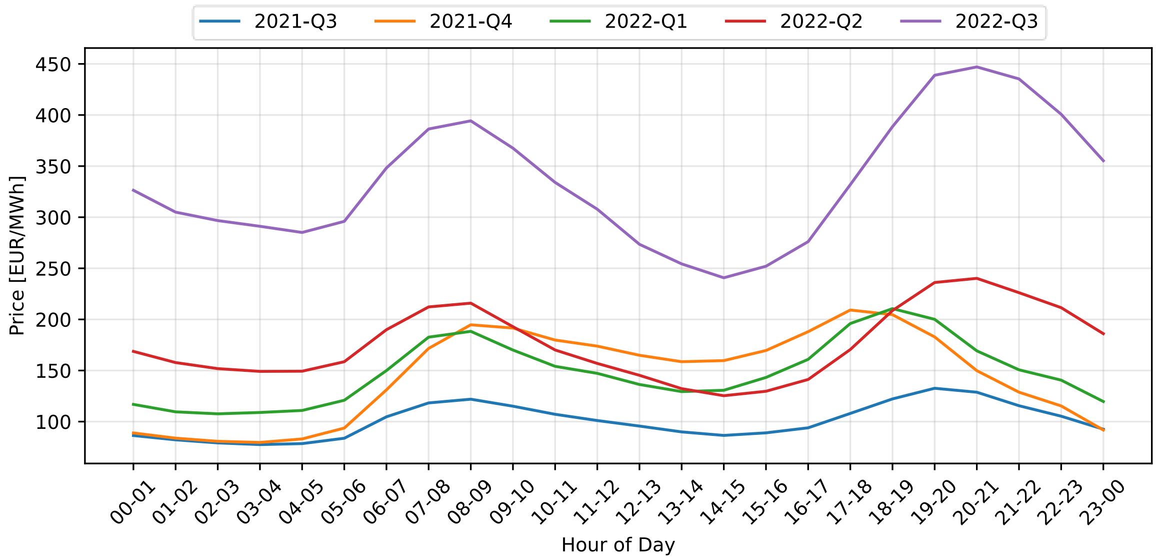

Figure 8: Average daily spot price profiles by quarter from July 2021 until September 2022.

2.2.5 Operating and investment expenditures

The assessment further compares expenditures – both operational and investment – for different system architectures. The considerations are made for four different layouts, presented in Figure 9. Scenario #1 considers a fast-charging station directly connected to the grid (no PV or BESS) with two EV connectors of 175 kW rated power each. Consequently, this setup requires a grid connection of 350 kW. Scenario #2 considers the combination of a fast-charging station with the 312 kWh BESS prototype, but without a PV system. The grid connection is chosen as 43 kW, thus, the same rating as for the actual setup on Bornholm. Scenario #3 comprises the HPC and a 61 kWp PV system, but without BESS. Hence, the setup requires a grid connection of 350 kW, as for scenario #1. Finally, scenario #4 is identical to the prototype installed on Bornholm, comprising the fast chargers, the BESS, the PV system, and a 43 kW grid connection.

The comparison of operating costs is done through a simulation study with each system architecture. The simulations were based on the actual PV and EV data recorded at the demonstration site. The time resolution of the simulations was set to 1-minute intervals.

The energy related operating costs are calculated using historical time series for spot prices [13], DSO tariffs [14], and TSO tariffs [15], and the simulated power profile at the grid connection point in the defined 1-minute resolution. The electricity costs for grid imports are calculated as

$$\Psi_{\text{import}} = \sum_{i=1} P_{import,i} \cdot \frac{1}{60}\text{h} \cdot (\psi_{spot,i} + \psi_{TSO,i} + \psi_{DSO,i}),$$

where i is the simulation time instance, $P_{import,i}$ is the import power, $\psi_{spot,i}$ is the spot price, $\psi_{TSO,i}$ is the TSO tariff, and $\psi_{DSO,i}$ is the DSO tariff. Similarly, the revenues from exporting energy to the grid are calculated as

$$\Psi_{\text{export}} = \sum_{i=1} P_{export,i} \cdot \frac{1}{60}\text{h} \cdot \psi_{spot,i},$$

where $P_{export,i}$ is the export power at simulation time instance i, and $\psi_{spot,i}$ is the spot price. Further details are based on the observed operating data of the prototype and are therefore provided in the following section.

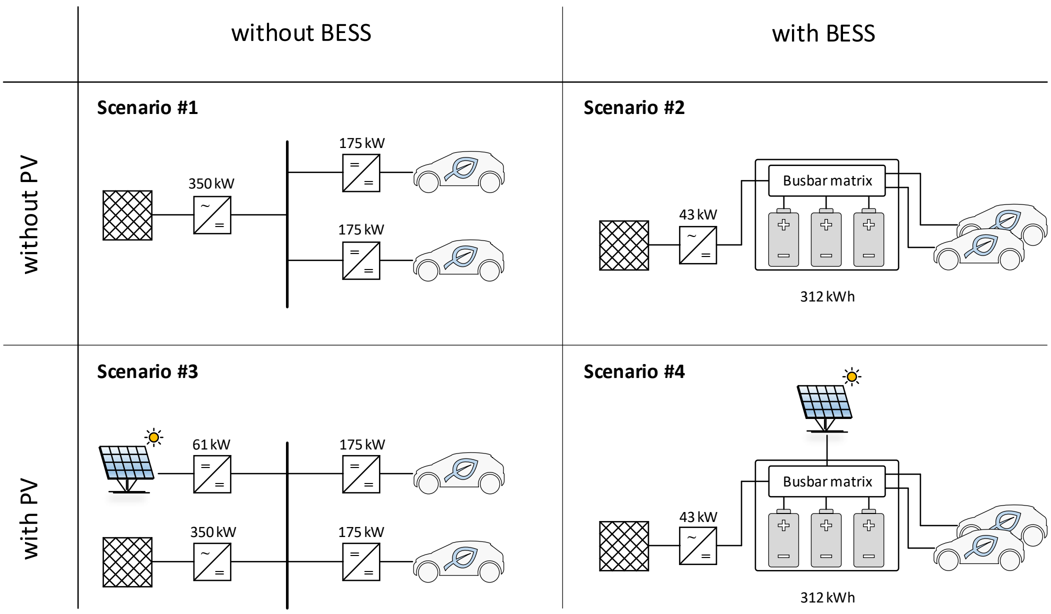

Figure 9: Overview of four different microgrid architectures. For each of the layouts both operational and investment expenditures are assessed.

The operating costs were determined through 1-year simulations between September 2021 and August 2022 with all four system setups, using actual PV and EV data recorded at the demo site.

The PV time series is based on measurements for a reference 61 kW PV system on the same rooftop (68.24 MWh per year), since the PV system connected to the prototype occasionally had to be curtailed when grid export was not approved yet. The EV consumption profile is based on August 2022 and repeated throughout the year, corresponding to a total EV consumption of 58 MWh/year. This month is chosen since it represents a period where all system functionalities were active. The simulation model for scenarios #2 and #4, both including the 312 kWh BESS, apply the same EMS logic used in the prototype on Bornholm. This allows for the reconstruction of the system operation with grid exports being enabled right after the deployment of the HCS. The simulation model also considers the battery roundtrip efficiency of 93.5%, as well as an average auxiliary consumption of 1.98 kW (17.4 MWh per year), which is based on the second-based power measurements for the prototype in August 2022. The calculation of energy related operational expenditure based on electricity costs for grid import and export were previously introduced in the methodology section.

Table 2 summarizes the operating costs and grid energy exchange for all four scenarios. The results show that scenario #1 has the highest energy costs. Scenario #2 has a higher imported energy compared to scenario #1, due to the corresponding power losses of the added BESS. However, the battery allows for importing energy when prices are low, and achieves overall lower energy costs. Scenario #3 shows that the local PV system makes the HCS less dependent on grid imports. Furthermore, the system also exports surplus energy to the grid, generating revenues in certain time periods. Overall, the import costs exceed the export revenues, leading to total annual energy costs of 3.47 kEUR. However, the total amount of both imported and exported energy is relatively high, signifying a low coincidence factor of PV and EV, since EV fast charging processes are commonly short but with high power intensity. This aspect underlines the potential of adding a BESS. Consequently, the results of scenario #4 show lower amounts of both import and export energy, due to the buffering effect of the storage system. Thus, costs for import and revenues for export are lower compared to scenario #3. With 1.29 kEUR, this scenario has the lowest annual operating costs for energy.

Table 2: Operating energy expenditures and revenues for different system architectures.

Scenario	E_{import} [MWh]	E_{export} [MWh]	Ψ_{import} [kEUR]	Ψ_{export} [kEUR]
Direct grid (#1)	77.05	-	17.75	-
Battery (#2)	79.14	-	14.96	-
PV (#3)	59.52	48.46	13.65	10.18
Battery + PV (#4)	56.42	42.42	9.63	8.34

The considered scenarios have distinct features in their respective system architectures. Scenario #4 shows the lowest operating costs but also includes more components. Although a complete economic comparison is out of scope for this paper, the following table provides an estimate of the investment costs for each of the four scenarios. These costs involve the capital expenditure for the individual components, as well as the required grid connection costs. The scenario with the lowest total investment costs is #1 with 124 kEUR, followed by #3 with 166.9 kEUR, which includes the PV system of 61 kWp. Scenario #2 entails the third-highest investment costs of 193.2 kEUR, including the costs for a 312 kWh battery system, while #4 has investment costs of 227.7 kEUR. These estimations show that the battery is the main driver of the high investment costs, but it conversely reduces operating costs significantly. Moreover, a grid connection of 350 kW may be too large in some locations, hence this table provides an estimation of required additional costs for architectures with a battery system. Finally, the demonstration on Bornholm showcased that battery-buffered fast charging stations may also be considered as a mobile solution that can be temporarily installed at key locations, until grid upgrades are in place.

Table 3: Capital expenditures for different system architectures.

Scenario	Grid connection costs [kEUR]	Battery costs [kEUR]	PV system costs [kEUR]	Converter costs [kEUR]	Total costs [kEUR]
Direct grid (#1)	75.0	-	-	49.0	124.0
Battery (#2)	9.4	177.8	-	6.0	193.2
PV (#3)	75.0	-	34.5	57.4	166.9
Battery + PV (#4)	9.4	177.8	34.5	6.0	227.7

3 Impact assessment for use case #5 – Local bio-based economies supporting the electrical, thermal and transport systems integrated management

The impact assessment for UC5 is structured in two main sections. Section 3.1 defines the KPIs relevant for this use case, split into operational flexibility of connected units, biogas and methanol production, as well as multi-energy coordination at the substation level. Subsequently, Section 3.2 evaluates the impact of UC5 based on the defined KPIs.

3.1 Definition of KPIs

The definition of KPIs is split into three parts covering (i) the operational flexibility of individual distributed generation units (such as wind turbines, biogas plants and photovoltaic installations), (ii) the biogas and methanol production, and (iii) the impact of increased multi-energy coordination between the units on a substation level. Relevant KPIs are listed and defined for these three parts.

3.1.1 Operational flexibility

For individual units in flexible operation, the following key technical flexibility characteristics are decisive [16]:

- Power and energy capacity (kW and kWh)
- Ramping rates (kW/s)
- Activation and deactivation delays (s)
- Accuracy and precision of the response (%)

Figure 10 visualises these characteristics in a stylised way in terms of power over time. The power and energy capacity are determined by the nameplate limits of the individual units, as well as by the weather conditions in case of renewable energy sources (wind and solar PV). The power capacity refers to the instantaneous physical power capacity, while the energy capacity to the amount of physical power over a certain time interval. The ramping rates define the transition between specific power setpoints, meaning the rate of change of power output from the units. The activation and deactivation delays are measurements in terms of time addressing the response time of specific units to setpoint changes. Accuracy defines the mean deviation of the response from the requested output, while precision details the variation span in the response. For an extensive overview of both technical and non-technical flexibility characteristics, the reader is referred to Degefa et al. [16].

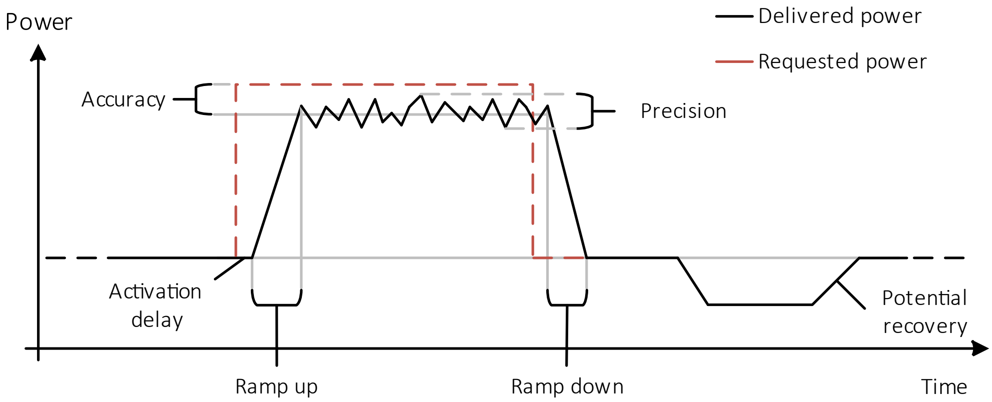

Figure 10: Main technical flexibility characteristics [17].

In the range of the demonstration activities in UC5, the controllability of different distributed generation units that are installed in the substation of Aakirkeby was investigated. The goal was to determine how well already installed units are following specific active power setpoints. This opens the possibilities for the implementation of joint control strategies as part of a VPP. Figure 11 locates the units under investigation around the 60/10 kV substation in Aakirkeby.

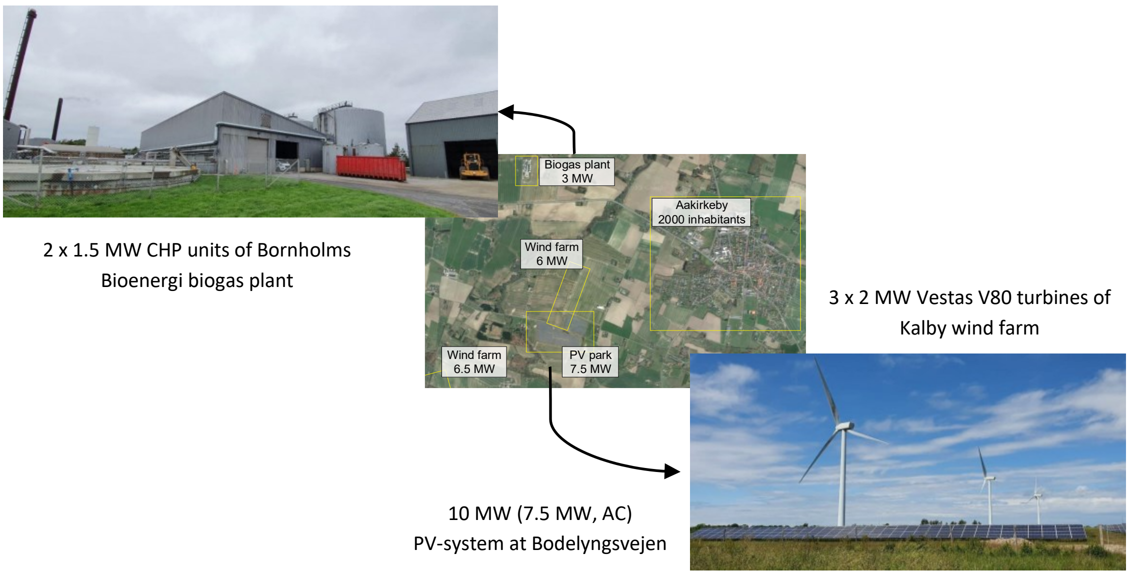

Figure 11: Overview of distributed generation units connected at the substation of Aakirkeby.

3.1.2 Biogas and methanol production

Examining the operation of the biogas plant more closely, important KPIs for energy and fuel production are defined:

- Available biomass (either ton or MWh of input)
- Amount of biogas generation (m^3 per day or month)
- Amount of electricity and heat production (MWh per day or month)

- CO_2 emissions (kg CO2)
- Potential methanol production (t or l of MeOH)

Currently, the biogas plant is treating local wastes from farming and animal husbandry for producing combined heat and power (CHP) [18]. In the future, it is envisioned to diversify the biogas applications by producing alternative fuels, such as methane or methanol, which can be used for heavy and seaborne transportation [17] [18]. Figure 12 provides a process overview for the biogas plant and methanisation processes in a block diagram, highlighting the mentioned KPIs.

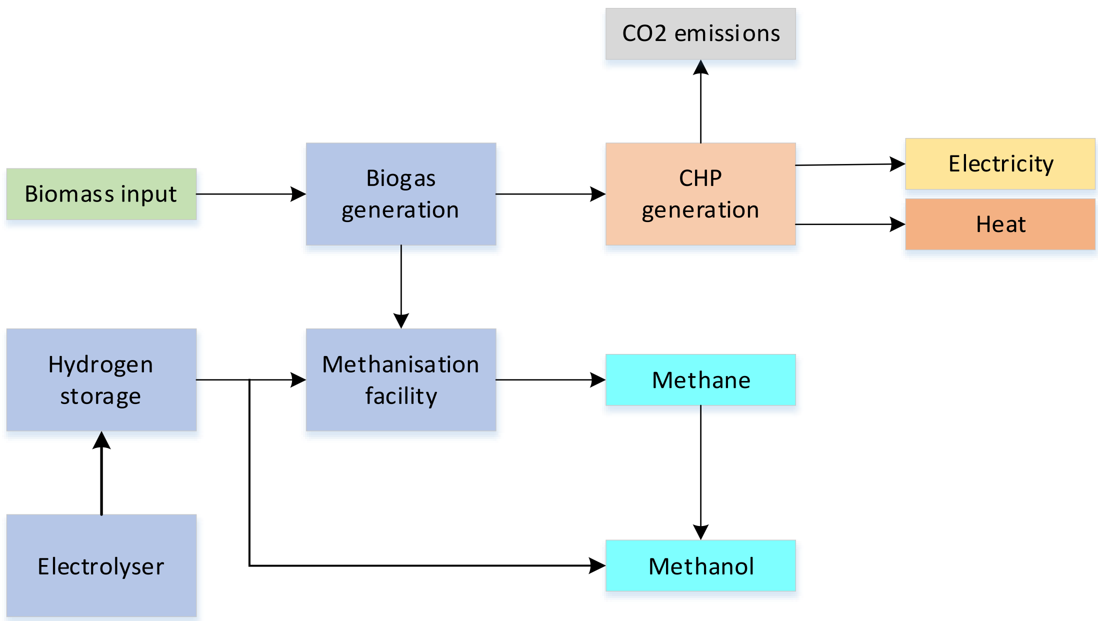

Figure 12: Process overview for a biogas plant with connected methanisation plant.

3.1.3 Multi-energy coordination at substation level

The third part of the assessment focuses on the coordination of distributed energy resources at a substation level. The key part of this investigation revolved around the sizing of hydrogen assets at the substation for producing green hydrogen that can be used to fuel the ferry connection between Rønne, Bornholm, and Ystad, Sweden. Relevant KPIs in this regard are:

- Share of RES in electricity production and curtailment (MWh_{el})
- Share of RES in heat production and curtailment (MWh_{th})
- Carbon emissions reduction (kg CO_2 avoided)
- Electrolyser and hydrogen storage size (MW and kg)
- Annual hydrogen production potential (t/year)

Figure 13 visualises the diverse set of units and their sizes connected to the electricity and district heating system of the substation in Aakirkeby. The figure highlights how hydrogen assets could be integrated into the electrical and thermal energy balance and what role they could play for decarbonising parts of the island where electrification is difficult to realise [19].

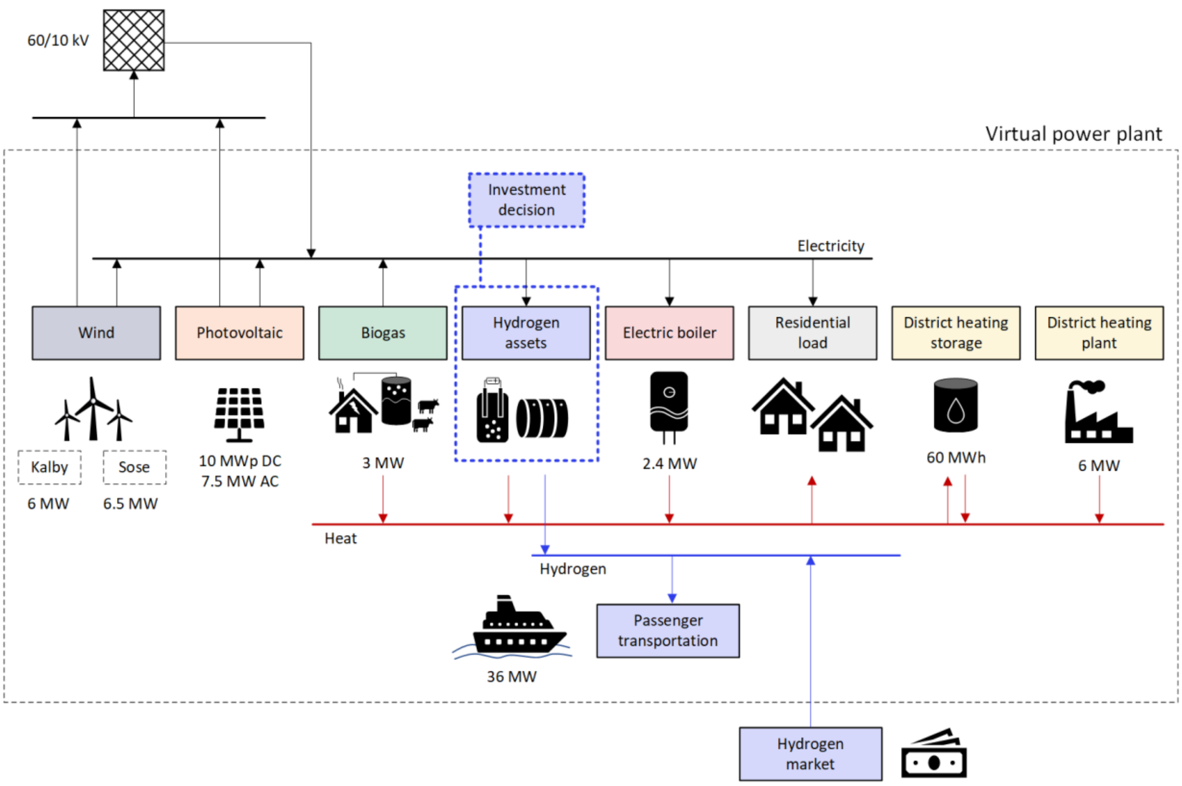

Figure 13: Overview of the units connected to Aakirkeby substation on Bornholm [17].

3.2 Evaluation of KPIs

3.2.1 Assessment of operational flexibility

In traditional power systems, the generation side typically adjusted its operation schedule to match varying demand over time: Centralised, dispatchable plants that are in general able to perform a fast output power modulation upon an imbalance in the supply-demand balance provide an appropriate response to system conditions. Traditional peak power plants, such as natural gas-fired units, are to be gradually replaced with RES and DERs that together can provide similar functionalities. Besides hydro power plants, other technologies are, for instance, dispatchable biomass-based plants [20]. For islanded systems, it mainly depends on the geographical circumstances which key system components depict the future, low-carbon generation side. For instance, some islands will rely predominantly on wind resources (e.g., Ireland, the Faroe Islands, and the Shetland Islands), while others might have access to geothermal resources (e.g., Iceland). With a focus on Bornholm, the work in this project focuses on biogas plants as dispatchable units, as well as wind and solar PV as low-carbon RES.

Table 4 provides an overview of the key performance indicators for operational flexibility from several experiments conducted with the distributed generation units operating on Bornholm. The table provides insights into how fast, accurate and precise the units react to active power downregulation requests that could, e.g., come from a distribution system operator (DSO) looking for securing the balance of demand and supply or addressing congestion in the network. The results show that the tested renewable distributed generation units perform satisfactorily [21].

Table 4: Overview of key performance indicators for operational flexibility for experimentally tested distributed generation units on Lighthouse Island Bornholm.

Key performance indicators	Wind farm	PV installations	Biogas plant
Max. power capacity	6 MW	7.5 MW / 115.6 kW	3 MW
Energy capacity	Depending on availability	Depending on availability	Depending on storage level (2500 m³)
Activation/deactivation	11 s	2 s	–
Accuracy (%)	0.01 (excl. spikes) 5.46 (incl. spikes)	0.08	0.15
Precision (%)	±0.6	< ±0.05	1

Flexible wind farm operation

The wind farm consists of three Type C Vestas-V80 turbines, each with a capacity of 2 MW, a rotor diameter of 80 m and a 60 m hub height. The wind farm has been installed in 2006 in the south-west of Aakirkeby, Bornholm, and lies now in immediate vicinity of the 10 MWp PV plant. Relevant parameters, such as active power, wind speeds at the nacelles, rotor speed and pitch angle, are measured in a second-by-second resolution for each of the three wind turbines and streamed to DTU's energy data hub (energydata.dk).

Figure 14 plots the active power (top plot), the wind speeds, the blade pitch angles, and the rotor speeds from the three wind turbines during the experiment. In the marked time windows, a power limitation request was sent to the three turbines to reduce their active power to 1000 kW in the first and to 500 kW in the second period. The pitch significantly increases during the power limitation, following an increase in generator speed, and thereby spilling excess power above the set cap.

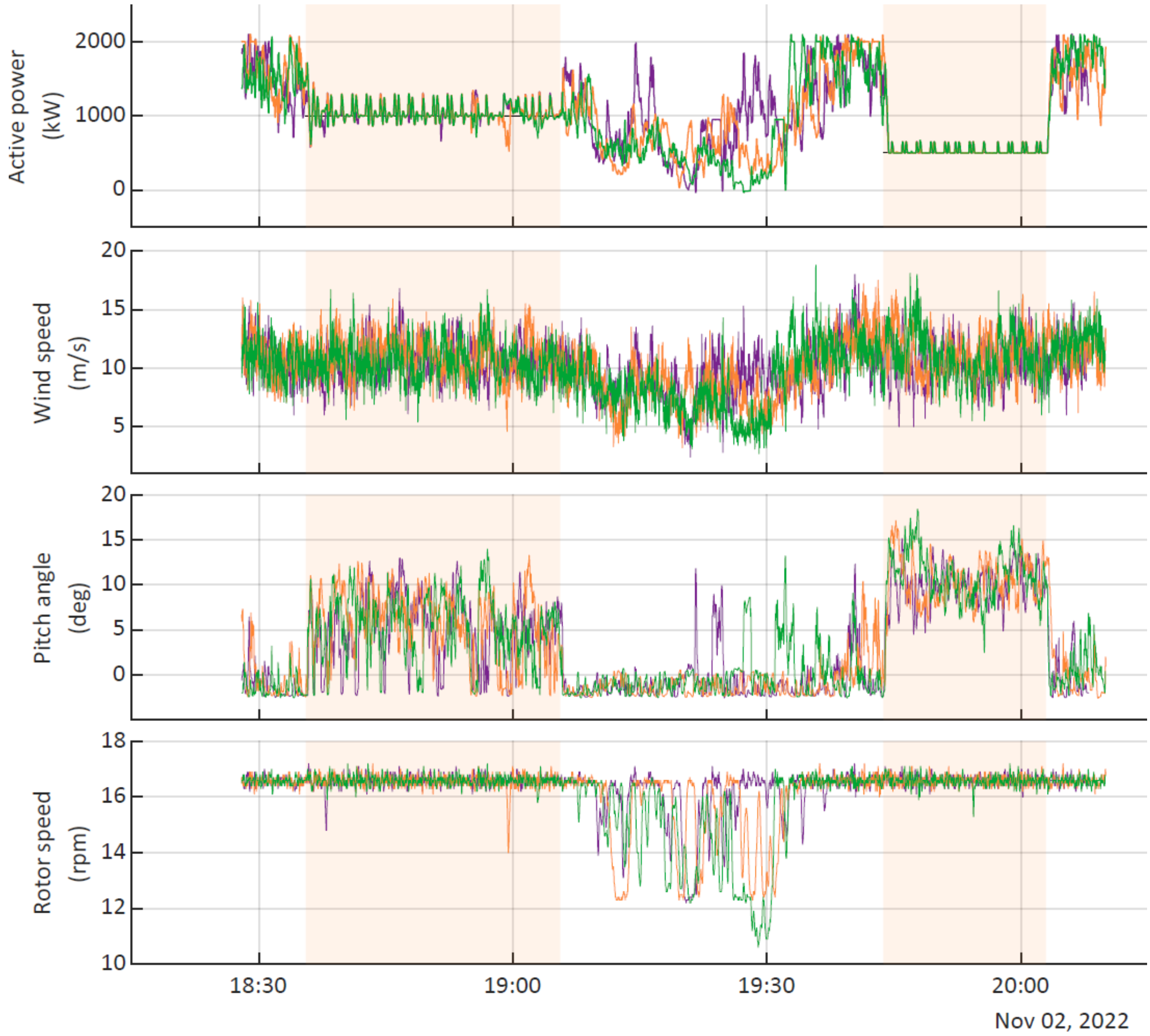

Figure 14: Measurements on active power, wind speeds, blade pitch angle and rotor speed from three wind turbines during the experimental power limitation tests (orange) on November 2, 2022 [17].

The general accuracy of the wind turbines' responses to the power limitation is good, although revealing recurring overshoots of up to 150 kW above the set limitation request. These overshoots last for 10-15 s before the output reverts to 500 kW. The origin of these deviations is most likely due to the power boost feature in the turbine controller, as has been confirmed by the manufacturer *Vestas*. The mean value of the response for the whole period including the recurring spikes is at 527.29 kW, signifying a deviation of 5.46% relative to the setpoint. When excluding the spikes, the response of the turbines is closely centred around 500 kW with a mean difference of 0.01% and a precision of ± 0.6%. After activation delays of 10-11 s, the turbines downregulated their active power with a ramp rate of 44.4kW/s, while upregulating back to fully available power with on average 60kW/s.

Flexible photovoltaic plant operation

Tests with two different PV systems were conducted. One with a 10 MWp PV system located in Aakirkeby, and one with a 116 kWp PV system located on Campus Bornholm in Rønne. The test with the second PV system was added due to the possibility of higher measurement detail. In fact, this is the remaining part of the PV system used in the demonstration activities of UC 4.

The PV plant is remotely controlled from the control room of the subsidiary company Bornholms Elproduktion A/S of the local DSO Bornholms Energi og Forsyning (BEOF). The goal of this experiment was to induce an absolute power limitation for approx. one hour in which the aggregated power production of the PV strings is first reduced to 60 kW (~33.33 % of the total inverter power of 180 kW) for half an hour and then further to 40 kW (~22.22 %) for the remaining time. The setpoints are given on the AC side of the inverter.

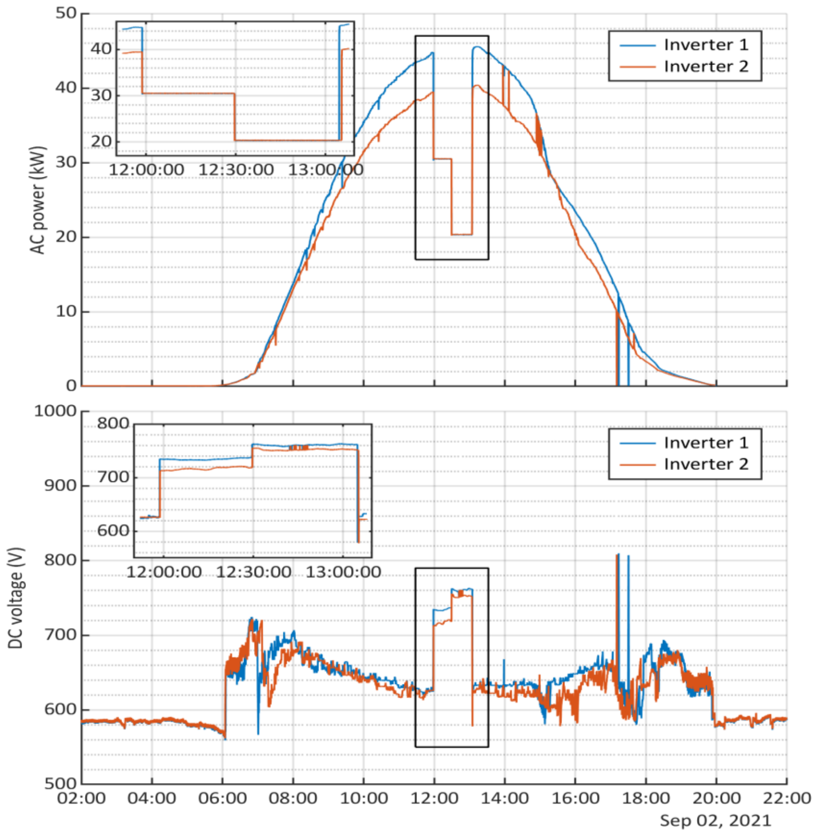

Figure 15: DC power and voltage measurements of a 115.8 kWp PV system for one day with power limitation period.

As can be seen from Figure 15, the inverters respond almost instantaneously to the power limitation request by increasing the operating DC voltage of the array. In this way, a suboptimal power point can be reached. The PV power during the limitation period reduces from 85 kW to 60 kW within 8 seconds after receiving the setpoint change order.

Flexible biogas plant operation

The biogas plant under investigation has a total electrical output power of 3 MW, split into two equally-sized *Jenbacher 420* CHP generators. The biogas plant is located west of Aakirkeby, Bornholm, and is mainly fed from biogas generated from agricultural wastes and animal residues. The plant represents a key element for providing dispatchable electricity generation in the renewable-dominated energy system of the island, as well as co-generated heat for the local district heating system. Previous studies and deliverables of the Insulae project have attempted to model this biogas plant, explain its functioning, and assess its possibilities for biogas upgrading [18],[22]. For this active power control experiment, the operator of the plant, Bornholm's Bioenergi ApS, agreed to follow a pre-defined power profile for two hours of continued operation. In this way, the ramp rates, accuracy and precision, as well as impact on thermal output and gas flows in the plant can be investigated. The data are gathered in a 2-second resolution and were provided by the plant operator after the experiment. Figure 16 reports the electrical and thermal output as well as gas flows during the APC of the biogas plant. The top plot of Figure 16 emphasises the capability of the plant to closely follow a given reference (black). Moreover, the ramp rates of the plant are visible when transitioning from one setpoint to another. The plant is changing its output from 950 kW to 1485 kW with a linear ramp rate of about 7 kW/s. This is on the lower end of what can be expected from these generators [23]. With ramp rates of around 7-8 kW/s, the biogas plant is also not strictly adhering to the specifications made in the applicable Danish grid code (TR 3.2.3). Therein, a ramp rate in between 10-300 kW/s is specified for thermal generators above 11 kW. However, to obtain approval for grid connection, the generators must generally be able to fulfil this requirement, and hence higher ramp rates may be obtained by changing the settings of the generator control.

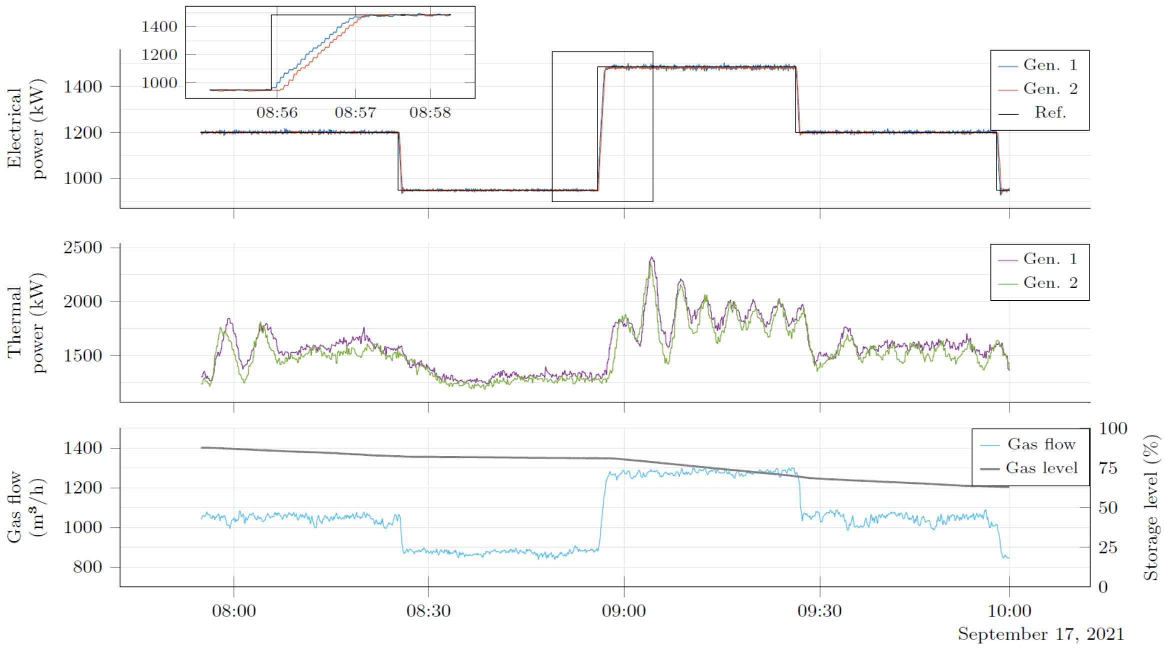

Figure 16: Measurements for active power, thermal power, and gas flows of a 3 MW biogas plant.

3.2.2 Assessment of biogas and methanol production

The biogas production process starts with the delivery of slurry from local farmers on Bornholm that live in close vicinity to the plant. Deliveries take place around 60 times a week on working days, i.e., around 12 deliveries each day from Monday to Friday, with an average driving distance of 13.8 km. One delivery comprises on average 36 tons of, e.g., animal slurry or slaughterhouse waste. The average price the biogas plant must pay is around 2 € per ton of slurry. By processing local organic waste, the biogas plant contributes to the island's decarbonization. In the current structure of the plant, the average substrate composition consists of 70.48 % cow slurry, 19.82 % of pig slurry, 6.17 % of slaughterhouse waste, 3.30 % of corn and 0.22 % of fish waste, with an average percentage of total solids in the feedings of 12–14 %. The island of Bornholm possesses a large feedstock potential (see Table 5) both from animal husbandry, household wastes and secondary crops which is currently not fully exploited: from a total estimated amount of 741,425 tons the biogas plant currently has a permission to treat only 120,000 tons per year [18].

Table 5: Overview of annual biomass potential and respective estimated energy content on the island of Bornholm.

Biomass	Potential	Energy content
Liquid manure	547,536	70,908
Straw	88,480	157,500
Wood chips	50,000	25,105
Deep litter	29,731	17,592
Garden waste	8,920	4,479
Other	16,758	8,674
Total	741,425	284,258

Figure 17 gives an overview of the simulated biogas production based on daily feedings, retrieved from the established biogas plant model presented in [22]. The top plot indicates the amount of organic feeding per day (in blue stars) as well as the monthly average to September 2020, based on real data from the biogas plant on Bornholm. The second plot shows the biogas production rates per feed, while the third plot aggregates these over time. The fourth subplot sums the different ongoing biogas production rates into total aggregated biogas production of all feeding instances. The range of 0.28–0.32 m^3/s corresponds to a gas flow rate of approximately 1008–1152 m^3/h, resulting in a daily biogas production of around 25,000 m^3 per day, and hence 750,000 m^3 per month. For a time horizon of 15 days, the aggregated cumulative biogas production amounts to 381,000 m^3.

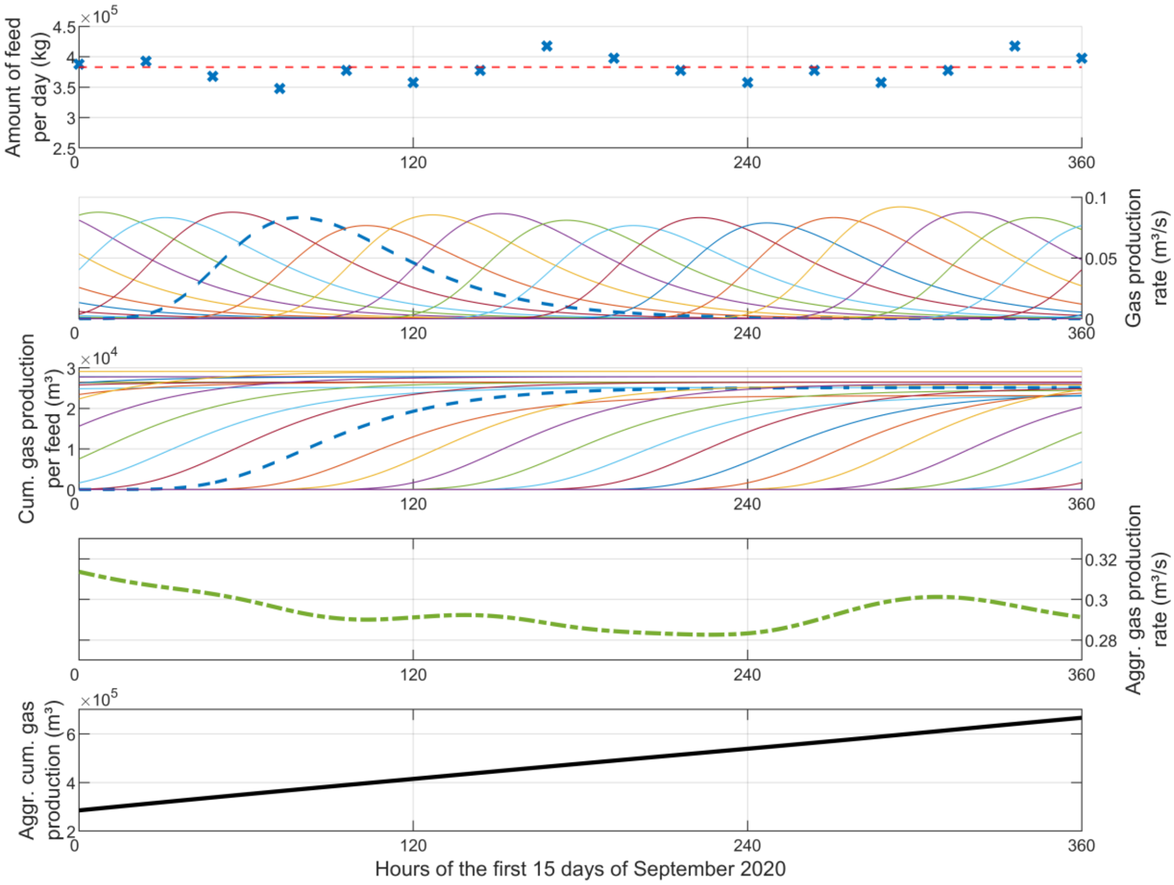

Figure 17: Simulated biogas production based on daily feedings into the digestion tanks [22].

Upgrading to synthetic natural gas (SNG) Apart from the low-carbon co-generation of electricity and heat, biogas plants can be used for upgrading biogas to synthetic natural gas (SNG) [24]. The generated SNG can hence be injected into the natural gas grid or liquefied for the transportation sector (e.g., heavy-road or maritime transport). Moreover, biogas plants represent a compelling site choice for power-to-gas and methanization facilities as they offer connections to DHNs which increases the energy efficiency of the conversion processes. Within the Insulae project, the role of a biogas plant is investigated as part of a multi-domain virtual power plant. This section analytically reviews the potential for biogas upgrading at the Bioenergi biogas plant on the island of Bornholm from a pure energy perspective. Due to its high efficiency at elevated temperatures and possible utilization of waste heat, the catalytic methanization of biogas via hydrogenation is examined. Based on a Sabatier reaction, biogas is enriched with hydrogen (H_2) for converting its share of carbon dioxide (CO_2) to methane (CH_4). The investigation and comparison of alternative upgrading technologies (e.g., CO_2 removal by physical or biological methods) has not been carried out in this project and remains for further research. A review of current and prospective biogas upgrading technologies has been performed by Angelidaki et al. [25].

Following the energy balance presented by the Danish Energy Agency and Energinet [26], a methanization process via the hydrogenation of biogas requires besides a small share of electricity (0.76 % of the input energy in MJ) a larger share of hydrogen (45.88 % of the input energy in MJ). The remaining 53.36 % of the input energy is stored in the biogas. If it is intended to transform the monthly biogas production of 750,000 m³ from the plant into SNG, approximately 121 tons of hydrogen and 67 MWh of electricity are needed, following the above stated ratio in terms of energy. The production of 121 tons of hydrogen requires in one month 6655 MWh of electrical energy, assuming an efficiency of 55 kWh/kg H_2 in an electrolysis process [27]. For one month of 30 days, this would require an electrolyser of 9.2 MW to run at nominal power throughout the whole month. Then, out of 750,000 m³ biogas, a total amount of 815,929 m³ of SNG may be produced. While the total energy that can be retrieved from 750,000 m³ of biogas with an assumed energy content of 6.5 kWh/m³ is 4875 MWh, the upgraded amount of SNG holds an energy content of approximately 8135 MWh, considering 9.97 kWh/m³. The energy content of the biogas corresponds to the energy requirement of the generators running at 95 % of nominal power throughout the month. From the produced SNG, only 62.7 % could be directly utilized in the generators running at full load. The remaining 37.3 % (3034 MWh; 304,349 m³) of the SNG production can be used either for transportation or other energy requirements. It is noteworthy that the gained 3034 MWh stored in the SNG in relation to the additional 6,655 MWh needed for the electrolysis process result in an efficiency of 45.59 % for this conversion process. The monthly energy requirement for the electrolysis process is three times higher than the biogas plant's electrical energy production. To this end, it would be important to couple the electrolysis process with surrounding large-scale renewable energy sources such as wind and PV farms where excess generation in case of grid overloading may be used for hydrogen generation. However, it is unlikely that this will result in a constant 9 MW power flow throughout the month.

Upgrading to methanol (MeOH) An alternative to the upgrading to SNG could be the upgrading to methanol (MeOH, chem.: CH3OH). Methanol is discussed as potential motor fuel, e.g. for ferries, to offset the use of CO_2-intensive diesel or marine diesel. As the largest shipping company worldwide, Mærsk has recently ordered new container ships with two-stroke engines running on methanol. For the sake of providing a reference, the amount of methanol that can be produced from the operation at Bornholm's Bioenergi biogas plant is investigated in this section.

It is assumed here that the CO_2 of the combustion process of biogas can be captured and re-utilised for methanol production. The combustion of 1 m³ biogas releases approximately 1.8 kg of CO_2. With a monthly production of biogas of 750,000 m³ and presuming that all biogas will be burned in the generators, a maximum amount of 1,350 t CO_2 will be released within one month. If presuming a 9 MW electrolyser to be installed on-site, analogously to the previous examination, approx. 120 t H_2 can be produced. Based on the mass balance, 120 t H_2 can react with 856.25 t CO_2 which corresponds to capturing 63.43 % of the CO_2 released from the burning process. Considering these input values, 625 t MeOH can be produced which corresponds with a density of 0.79 kg/l to 791,139 litres of MeOH. The electrical energy needed for the electrolysis – approx. 6,655 MWh. Methanol has an energy content of 16 MJ/l. Hence, the produced 791,139 litres of

MeOH hold 3,516 MWh, being around 53 % of the input energy.

To give a reference of the potential offset of marine diesel in the case of Bornholm, the produced methanol is compared with the energy requirement of the ferry connecting Bornholm with the mainland of Sweden. The seaborne passenger transportation is a large contributor to the island's GHG emissions. The ferry is equipped with four MAN 20V 28/33D engines, each with a nominal power of 9 MW and a specific fuel consumption at full load of 193 g/kWh. The total engine power of the 112.6 m long and 30.5 m wide ferry is hence 36 MW. Considering an average loading of 60 % of the nominal power for an 80-minute one-way trip, the energy consumption of one engine amounts to approximately 7.2 MWh. With the given specific fuel consumption, this value corresponds to 1.39 t fuel for one engine. Considering an energy density of 0.9 kg/l and all four engines, this would give a fuel consumption of 6176 litres for one crossing. On a daily basis seen for the whole year, the ferry travels back and forth around five times, signifying 10 crossings in total. The daily fuel consumption of 10 crossings would then correspond to 55.6 t diesel fuel. In a month, approximately 1668 t of fuel are consequently used for the seaborne passenger transportation from and to the island of Bornholm. As calculated above, around 625 t of MeOH may be produced from the biogas. Considering that MeOH with around 16 MJ/kg has a lower energy content than marine diesel (42 MJ/kg), approximately 2.6 times the amount of MeOH must be used in the ferries for the same energy requirement. This would result in a requirement of 4337 t of MeOH to substitute the monthly requirement of the ferry. The 625 t MeOH produced at the ferry would hence provide only a share of 14.41 %. In other words, the ferry could be fuelled only in 4.3 out of 30 days in a month with the generated MeOH – presuming that a one-to-one transition of fuel in the ferry's engines is possible. Aiming to fuel only the five trips going from Bornholm to the mainland, the generated MeOH can accordingly cover a share of 28.82 %.

3.2.3 Assessment of multi-energy coordination at substation level

The seaborne passenger transportation from and to the mainland is responsible for the largest share of Bornholm's emissions. Considering the goal of decarbonising this means of transportation from the island, as set out by the regional municipality of Bornholm, it is imperative to look at the CO_2 emissions connected to a specific intervention. Figure 18 reports the annual marginal CO_2 emissions for the one-way ferry connection between Rønne, Bornholm, and Ystad, Sweden, when using different fuel sources. The left bar of the figure represents the aggregated CO_2 emissions of 29.8 kt of emitted CO_2 for the case when diesel is used as fuel in the ferries. Here, it is assumed that 2.4 kg of CO_2 are emitted when burning 1 litre of diesel. The second bar on the left signifies the emissions connected with hydrogen that solely originates from conventional steam methane reforming (SMR), so-called grey hydrogen. Following Bareiß et al., direct CO_2 emissions of 8.8 kg occur in the production of 1 kg of H_2 [28]. Due to the higher energy content of H_2 compared to diesel, smaller amounts are needed to supply the energy demand of the ferry, leading to an overall reduction in marginal emissions of 14.5% (25.5 kt CO_2). However, SMR does not depict a genuinely sustainable option to produce hydrogen and should hence be replaced to the largest possible extent by green hydrogen production. When considering the contribution of green hydrogen that can be produced locally from this one substation on the island based on the presented investment decisions of this paper, the CO_2 emissions can be further reduced to 19.9 kt CO_2, i.e., by 22% and 33.2% compared to using only hydrogen from SMR or diesel, respectively. It is assumed here that the remaining hydrogen bought from a hydrogen market originates solely from SMR and is hence still associated with significant CO_2 emissions. In the future, the ramp up of green hydrogen production either at Bornholm, e.g., at other substations in a similar manner as presented in this deliverable, or on the retail market will lead to cases with higher percentages of green hydrogen. The two bars on the right indicate the CO_2 emissions connected to the theoretical cases when instead of 21.8% either 50% or 75% of the hydrogen demand of the ferry are met by green hydrogen. Compared to the case when using diesel, this means a reduction of emissions by 57.4% or 78.6 %, respectively.

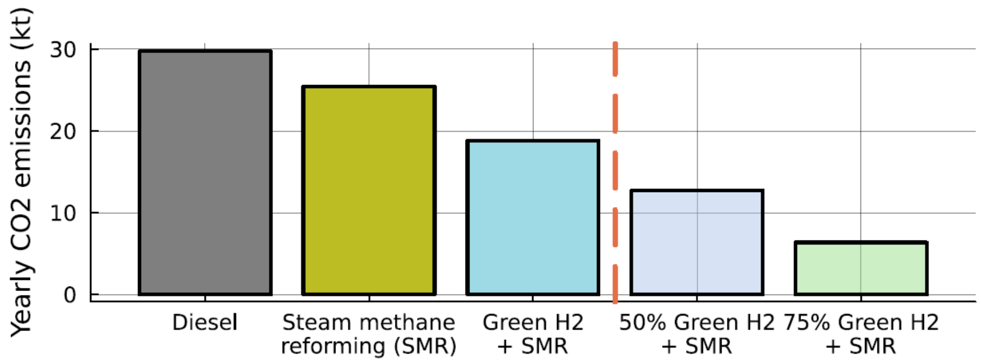

Figure 18: Yearly CO_2 emissions from different fuel sources and for specific targets of green hydrogen levels [29].

With a model-based analysis, an appropriate size for hydrogen assets has been determined for the substation of Aakirkeby on Bornholm. Considering the explicit hydrogen demand for the passenger transportation on the island of Bornholm, the model invests into an electrolyser system of 9.63 MW and a hydrogen storage of 1.45 t. From a power perspective, the size of the electrolyser corresponds to 52 % of the maximum residual power output (18.5 MW) at the substation within the sizing period from 2017 – 2019. The system is hence not scaled to harvest the peak power values, but rather to capture the large bulk of the overproduction.

The sized electrolyser is shown to integrate well into the multi-energy demand and supply balances at the substation. In particular, the recovered heat from the electrolyser system is a crucial supplement for the district heating system, adding to the heat production from the biogas plant, the electric boiler, and the district heating plant. The heat production of the electrolyser was found to supply a share of 21.4 % of thermal demand in this district heating system, either directly or indirectly through the thermal storage tank. The biogas plant contributes largest to meeting thermal demand at the substation with a share of 65.8 %, while the electric boiler and the district heating plant provide 14.3 % and 0.3 %, respectively. The latter two are exclusively used in winter months, due to their limited applicability and the higher heat demand. In a reference case with no hydrogen assets, the heat demand is mainly supplied by the biogas plant (64.1 %), followed by the electric boiler (37 %) and the district heating plant (0.2 %). The additional heat produced by the electrolyser system hence mainly influenced the operation of the electric boiler, due to the added value of the electrolyser system of producing hydrogen as well.

Seen for the whole period 2017–2019, 26 % of the total H_2 demand for passenger transportation from the island can be supplied by the invested hydrogen assets. The corresponding yearly average H_2 production that could be achieved by an electrolyser system of the determined size in this specific setting is 819.3 tons. Figure 19 shows the monthly hydrogen production throughout the three years under investigation. From this production pattern, no clear trend of seasonality can be identified. The spring months entail high H_2 production, due to high complementary production of wind and solar, whereas H2 production is low in winter for periods with low wind power.

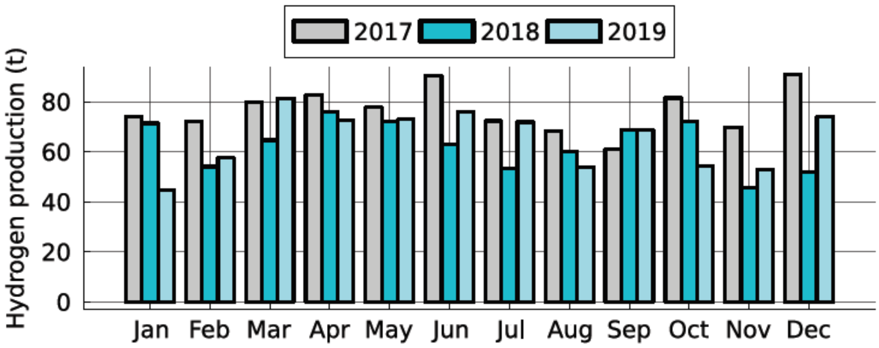

Figure 19: Monthly H_2 production throughout the years 2017–2019 [29].

4 CONCLUSIONS

For UC4, the demonstration results of a DC microgrid providing electric vehicle fast charging were presented. The setup, which was operational on the Danish island of Bornholm, comprises a novel type of battery system (312 kWh), two 175 kW EV fast chargers, a 61 kWp PV installation, and a 43 kW connection to the local AC distribution grid. The results showcase the feasibility of the system design which is largely reliant on the modularity of the battery system. The use of this battery technology, which has the intrinsic capability of reconfiguring its cell topology during operation, eliminates the need for DC-DC conversion stages between the connected units. At the same time, the system enables EV fast charging at limited grid connection points, while reducing the grid dependency and promoting local use of PV energy. Over the entire demonstration phase with this hybrid charging station (HCS), 2008 EV charging sessions were recorded, amounting to a total charged energy of 21.8 MWh. An overall proportion of 37.7% of the energy delivered to EVs was provided by the local PV system, defining the system's self-sufficiency. Furthermore, 90% of the total energy provided by the local PV system was utilized for EV charging, defining the system's self-consumption. The operational CO_2 emissions of the HCS amounted to $2092\ \mathrm{kg}_{\mathrm{CO}_2}$, which is a reduction of around 1 ton CO_2 compared to a charging system without local PV system ($3{,}094\ \mathrm{kg}_{\mathrm{CO}_2}$), and a reduction of 14.5 tons CO_2 compared to the emissions caused by ICE vehicles ($17{,}649\ \mathrm{kg}_{\mathrm{CO}_2}$). The analysis of the recorded timeseries demonstrated that the energy management system of the HCS specifically utilized time windows of low spot prices to import energy in periods of low PV production or high EV demand. Consequently, the presence of the BESS was used effectively to reduce the annual operating energy expenditures of the HCS to 1.29 kEUR. In comparison, the annual costs of a fast charger with a direct grid connection, without PV and BESS, were estimated at 17.75 kEUR. However, the HCS entails higher capital expenditure due to higher component costs.

The demonstration phase with the HCS prototype on Bornholm showed that, while the design is promising, there are several potential improvements to be made, in particular with respect to the EMS. One control challenge of the tested system design is the coordination of three battery strings with four potential units, which leads to compromises in the operation, and requires different prioritization of energy components. How this control challenge can be tackled was investigated in a follow-up study, using operational data from the prototype [30]. All in all, the demonstration activity showed that the developed prototype is a versatile solution, which facilitates renewable-powered EV fast charging with limited grid connection. The tested HCS design may also be employed as a mobile solution that can be temporarily installed at key locations, accelerating the roll-out of fast chargers until necessary grid upgrades are realized.

From the analyses in UC5, we can conclude with the following lessons learned regarding the active power control capabilities of distributed generation units. Distributed generation units can regulate their active power fast and with high accuracy and precision. Biogas plants are slower than PV inverters and wind turbines, but at the same time entail higher flexibility potentials without spilling instantaneous available energy. Already with today's technology standards, distributed generation units can be gathered into a VPP for jointly addressing flexibility requests from network operators. Yet, the coordination and potential communication delays between diverse units requires further investigations. The correct tuning of internal plant controllers for flexible operation is crucial to avoid undesired dynamics or spikes in the active power response.

If methanol or other synthetic e-fuels were to be produced in the VPP, the amount provides only a smaller share of future needs for an island. As one of the biggest contributors of CO_2 emissions, the ferry connection between an island and the mainland could be a potential candidate for the application of methanol. For the Bornholm case, it has been shown that the VPP could only produce a small share of 28.82 % for the trips leaving the island. In other words, this would correspond to be able to fuel one out of four ferries leaving on a daily basis. Moreover, this necessitates massive investment into chemical processing and hydrogen infrastructure around the biogas plant.

Hydrogen is envisioned to help decarbonising sectors where the direct electrification is difficult to realise. In UC5, we further investigated the optimal sizing of hydrogen assets for the VPP in Aakirkeby, Bornholm. We find that hydrogen assets can play a significant role in supplying the thermal district heating demand, while acting as flexible demand-side resource in the electrical domain. Specifically, a 9.63 MW electrolyser with a connected 1.45 t hydrogen storage account for 21.4 % of the annual district heating demand. Locally in the VPP, around 820 tons of H_2 could be produced from excess renewable production over the course of a year. This represents a share of 26 % of the yearly hydrogen demand of the ferries if they were to be powered by hydrogen fuel cells. The hydrogen market price strongly influences the dimensioning of hydrogen assets: If hydrogen can be bought centrally at prices below 3 €/kg, an investment into such assets does not seem economically viable. Higher electricity spot prices would increase this threshold, and vice versa. To sum up, green hydrogen production is not yet cost-competitive with other forms of hydrogen production. Policy makers should provide financial incentives for businesses to invest in green hydrogen technologies and infrastructure.

REFERENCES

[1] T. Gabderakhmanova, J. Engelhardt, J.M. Zepter, T. Meier Sørensen, K. Boesgaard, H. H. Ipsen, M. Marinelli, "Demonstrations of DC Microgrid and Virtual Power Plant Technologies on the Danish Island of Bornholm," Universities Power Engineering Conference (UPEC), 2020 Proceedings of the 55th International, pp. 1-6, Torino, 1-4 Sep. 2020.

[2] J. Engelhardt, J. M. Zepter, T. Gabderakhmanova, and M. Marinelli. "Efficiency Characteristic of a High-Power Reconfigurable Battery with Series-Connected Topology." In: Proceedings of the 2022 International Power Electronics Conference, IEEE, pages 2370–2376.

[3] J. Engelhardt, J. M. Zepter, T. Gabderakhmanova, G. Rohde, and M. Marinelli. "Double-String Battery System with Reconfigurable Cell Topology Operated as a Fast Charging Station for Electric Vehicles." In: Energies 14.9 (2021), page 2414.

[4] J. Engelhardt, T. Gabderakhmanova, G. Rohde, M. Marinelli, "Reconfigurable Stationary Battery with Adaptive Cell Switching for Fast-Charging of Electric Vehicles," Universities Power Engineering Conference (UPEC), 2020 Proceedings of the 55th International, pp. 1-6, Torino, 1-4 Sep. 2020.

[5] J. M. Zepter, J. Engelhardt, T. Gabderakhmanova, and M. Marinelli. "Re-Thinking the Definition of Self-Sufficiency in Systems with Energy Storage." In: Proceedings of the 2022 International Conference on Smart Energy Systems and Technologies (SEST), IEEE, pages 1–6.

[6] R. Wolbertus and R. van den Hoed, "Fast Charging Systems for Passenger Electric Vehicles," Energies, vol. 11, no. 4, p. 73, 2020.

[7] J. Engelhardt, Reconfigurable Batteries in Electric Vehicle Fast Chargers: Towards Renewable-Powered Mobility. Risø, Roskilde, Denmark: DTU Wind and Energy Systems, 2022. 150 p. doi: 10.11581/dtu.00000254.

[8] A. Thingvad, P. B. Andersen, T. Unterluggauer, C. Træholt and M. Marinelli, "Electrification of personal vehicle travels in cities - Quantifying the public charging demand," eTransportation, vol. 9, p. 100125, 2021.

[9] E. ToolBox, "Combustion of Fuels - Carbon Dioxide Emission.," 2009. [Online]. Available: https://www.engineeringtoolbox.com/co2-emission-fuels-d_1085.html.

[10] N. E. H. Jensen, Energinet, 19 01 2022. [Online]. Available: https://energinet.dk/Om-nyheder/Nyheder/2022/01/19/CO2-udledning/.

[11] A. Louwen, W. van Sark, A. Faaij and R. Schropp, "Re-assessment of net energy production and greenhouse gas emissions avoidance after 40 years of photovoltaics development," Nature Communications, vol. 7, p. 13728, 2016.

[12] A. Bowen, J. Engelhardt, T. Gabderakhmanova, M. Marinelli and G. Rohde, "Battery Buffered EV Fast Chargers on Bornholm: Charging Patterns and Grid Integration," in 2022 57th International Universities Power Engineering Conference (UPEC), Istanbul, Turkey, 2022.

[13] Energinet, 2023. [Online]. Available: https://www.energidataservice.dk/tso-electricity/Elspotprices.

[14] Trefor El-net Øst, 2023. [Online]. Available: https://www.trefor.dk/globalassets/mediebibliotek-trefor/3.-elnet/filer/historiske-priser/trefor-el-net-ost---priser-1.-april-2016---8.-januar-2023.pdf.

[15] Energinet, 2023. [Online]. Available: https://energinet.dk/el/elmarkedet/tariffer/aktuelle-tariffer/.

[16] M. Z. Degefa, I. B. Sperstad, and H. Sæle, "Comprehensive classifications and characterizations of power system flexibility resources," Electric Power Systems Research, vol. 194, p. 107022, 2021, doi: 10.1016/j.epsr.2021.107022.

[17] J. M. Zepter, Flexibility of Distributed Energy Resources in Islanded Multi-Energy Systems. Risø, Roskilde, Denmark: DTU Wind and Energy Systems, 2022. doi: 10.11581/dtu.00000255.

[18] J. M. Zepter, T. Gabderakhmanova, K. M. Andreasen, K. Boesgaard, and M. Marinelli, "Biogas plant modelling for flexibility provision in the power system of Bornholm island," in 55th International Universities Power Engineering Conference (UPEC), Torino, Italy, 2020, pp. 1–6.

[19] A. Barney, H. Polatidis, and D. Haralambopoulos, "Decarbonisation of islands: A multi-criteria decision analysis platform and application," Sustainable Energy Technologies and Assessments, vol. 52, p. 102115, 2022, doi: 10.1016/j.seta.2022.102115.

[20] O. M. Babatunde, J. L. Munda, and Y. Hamam, "Power system flexibility: A review," Energy Reports, vol. 6, pp. 101–106, 2020, doi: 10.1016/j.egyr.2019.11.048.

[21] J. M. Zepter, J. Engelhardt, M. Ledro, T. Gabderakhmanova, and M. Marinelli, "Experimental assessment of active power control of distributed generation units," Sustainable Energy Technologies and Assessments, vol. 60, p. 103500, 2023, doi: 10.1016/j.seta.2023.103500.

[22] J. M. Zepter, J. Engelhardt, T. Gabderakhmanova, and M. Marinelli, "Empirical Validation of a Biogas Plant Simulation Model and Analysis of Biogas Upgrading Potentials," Energies, vol. 14, no. 9, p. 2424, 2021, doi: 10.3390/en14092424.

[23] Clarke Energy, Electricity Peaking Plants, accessed: February 7, 2022. URL https://www.clarke-energy.com/us/applications/peaking-station-peak-lopping-plants/

[24] M. Götz et al. "Renewable Power-to-Gas: A technological and economic review." In: Renewable Energy 85 (2016), pages 1371–1390. doi: 10.1016/j.renene.2015.07.066.

[25] I. Angelidaki et al. "Biogas upgrading and utilization: Current status and perspectives." In: Biotechnology advances 36.2 (2018), pages 452–466. doi: 10.1016/j.biotechadv.2018.01.011.

[26] Danish Energy Agency and Energinet. "Technology data for renewable fuels: Technology descriptions and projections for long-term energy system planning." In: Catalogue on technologies for energy carrier generation and conversion (2017 (updated 2020)). url: https://ens.dk/sites/ens.dk/files/Analyser/technology_data_for_renewable_fuels.pdf.

[27] A. Buttler and H. Spliethoff. "Current status of water electrolysis for energy storage, grid balancing and sector coupling via power-to-gas and power-to-liquids: A review." In: Renewable and Sustainable Energy Reviews 82 (2018), pages 2440–2454. doi:

10.1016/j.rser.2017.09.003.

[28] K. Bareiß et al. “Life cycle assessment of hydrogen from proton exchange membrane water electrolysis in future energy systems.” In: Applied Energy 237 (2019), pages 862–872. doi: 10.1016/j.apenergy.2019.01.001.

[29] J.M. Zepter, J. Engelhardt, and M. Marinelli, “Optimal Expansion of a Multi-Domain Virtual Power Plant for Green Hydrogen Production to Decarbonise Seaborne Passenger Transportation.” Available at SSRN: http://dx.doi.org/10.2139/ssrn.4528069

[30] J. Engelhardt, S. Grillo, L. Calearo, M. Agostini, M. Coppo, M. Marinelli, “Optimal control of a DC microgrid with busbar matrix for high power EV charging.” Electric Power Systems Research. 2023;224:109680. doi: 10.1016/j.epsr.2023.109680